RECEIVED
OCT 0 8 1997
OSTI

ORNL/CP-94439

CONF-9709100--

Assessment of Effects of Neutrals on the Power Threshold for L to H Transitions in DIII-D

L W Owen†, B A Carreras†, R Maingi†, P K Mioduszewski†, T N Carlstrom‡ and R J Groebner‡

†Oak Ridge National Laboratory, Oak Ridge, Tennessee 37831
‡General Atomics, San Diego, California 92186-9784

Abstract. To assess the effect of edge neutrals on the low-to-high confinement transition threshold, a broad range of plasma discharges has been analyzed. From this analysis, the transition power divided by the density, at constant magnetic field, appears to be a function of a single parameter measuring the neutrals' effect. This parameter cannot be uniquely identified. For instance, it may be the radial decay length of the neutral profile or the charge-exchange damping rate at about $r/a \approx 0.95$. This results suggest that there is a missing parameter linked to the neutrals in the power threshold scaling laws.

1. Introduction

One of the characteristic properties of the transition from the low confinement mode (L-mode) to the high confinement mode (H-mode) [1], [2] is a power threshold. From the early experiments, the power threshold, P_{th}, generally increases with line-averaged electron density, $\bar{n}$, and magnetic field, B [3]-[5]. A scaling law of the form $P_{th} \propto \bar{n}B$ was proposed [6]. This scaling is found for single null divertor configurations with the ∇B direction towards the X-point. A power-threshold database exists from several devices operating in conditions similar to those of the present International Thermonuclear Experimental Reactor (ITER) design. These data permit the refinement of this scaling law, and variants have been obtained by requiring dimensionally correct parametric dependences and by including the device size dependence [7],[8]. However, there is not yet a scaling law that describes the data well enough to allow an extrapolation to ITER conditions with reasonable certainty. The observed variability of the power threshold with the wall conditioning in many devices suggests that atomic physics may be important.

Evidence for the importance of atomic physics effects surfaced in the first experiments that showed that access to the H-mode requires careful wall conditioning and a reduction in the wall recycling [9]. It is also well known that changes in wall conditioning and configuration can cause significant changes in the power threshold [10]. However, there is very little information on how wall conditioning affects the low to high L-to-H transition. An obvious potential mechanism is the coupling of the neutral dynamics to the transition mechanism, as indicated in several experiments [11]-[14]. Theoretical models have included the effect of neutrals on the L-to-H transition dynamics [15]-[19]. One of the main mechanisms is the change of the ion momentum balance through charge exchange friction.

Research sponsored by the Office of Fusion Energy, U.S. Department of Energy, under contract DE-AC05-96OR22464 with Lockheed Martin Energy Research Corp and DE-AC03-89ER51114 with General Atomics.

In this paper, we report the results of an analysis of the effect of the neutrals on the L-to-H transition experiments carried out in DIII-D Tokamak [20]. We have reconstructed the neutral distribution prior to the transition by combining measurements at the plasma edge, scrape-off-layer (SOL), and divertor with two-dimensional (2-D) modeling of these regions [21]. Having computed the neutral density, it is possible to calculate some key neutral parameters, such as energy loss and poloidal velocity damping rates. We have considered a broad range of plasma discharges with varying conditions: gas puff and pumping rates, position of the X-point, and line-averaged density. These different conditions give a highly scattered set of values for the power threshold when plotted versus line-averaged electron density at a constant magnetic field [20]. From the present analysis, a clear correlation has emerged between the charge exchange damping rate (or neutral density) in the edge region ($r/r_S \approx 0.95$, where r is the averaged minor radius of a flux surface and r_S the averaged minor radius of the separatrix) and the power threshold data.

2. Analysis of the gas puff, pumping, and density scan experiments

The data used in this analysis is a subset of discharges from two power threshold experiments performed in DIII-D as part of the ITER physics studies [8]. Both scans were carried out at fixed toroidal magnetic field $B = 2.1$ T. All these discharges are lower single-null divertor discharges with the shaping parameters similar to the ITER shape and the ion ∇B drift toward the X-point.

The first experiment, which was performed in 1994, is a power threshold density scan [22]. The power threshold is defined as the power through the separatrix, $P_{\rm sep}$, at the moment of the transition. It is calculated as $P_{sep} \equiv P_{NBI} + P_{Ohm} - P_{rad} - dW/dt$ where $P_{\rm NBI}$ is the power deposited by neutral beam heating, $P_{\rm Ohm}$ is the ohmic power ($P_{\rm Ohm} = I_{\rm p}V_{\rm surf} - dW_{\rm B}/dt$, where $I_{\rm p}$ is the plasma current, $V_{\rm surf}$ is the surface voltage, and $W_{\rm B}$ is the energy stored in the magnetic field), $P_{\rm rad}$ is the radiated power within the separatrix, and the last term is the rate of change in the total plasma energy. The power threshold dependence on line-averaged density has the characteristic shallow U-shape observed in several devices.

The second experiment that we analyzed corresponds to a set of DIII-D discharges carried out in 1996 to test the neutrals' effects on the power threshold [20]. To do so, similar discharges were run under varying conditions. Three variants were tried with the intention of changing the neutral density without changing the plasma parameters too much. A first set of discharges was run with a strong gas puff from the top of the machine to increase the ratio of neutral to electron density. A second set of discharges was run with the cryopump on, with the goal of decreasing the neutral density. Finally, as another way to increase the neutral density near the X-point, a set of discharges was carried out with the X-point moved closer to the target plate. The power threshold for the discharges with the cryopump on is 70% larger than that for the gas puff discharges, and the densities are about 20% to 40% lower. The results of this experiment seem to be counter-intuitive, with the discharges for which the goal was to increase the neutral density having lower power threshold than the ones for which the goal was to decrease it.

In the procedure adopted for this work, the analysis of the data involves two steps. Since the neutral density distribution at the plasma edge is not measured, we first reconstruct the neutral density and temperature distributions and the corresponding plasma-neutral reaction rates. The second part of the analysis is the evaluation of parameters that may characterize the role of neutrals in the L-to-H transition, such as the charge exchange damping rate, ν_{CX}, and the neoclassical poloidal flow damping rate, μ_{neo}. The primary numerical tools used in the reconstruction of the neutral density distribution are the B2.5 code [23], a 2-D multifluid edge plasma transport code, and the DEGAS code [24], a 3-D Monte Carlo neutral particle transport code. These two codes are used iteratively but not coupled. Details of the analysis are given in Ref. 21.

The calculated density profiles of neutrals in the SOL show that the neutral density responded as expected in the experiment. That is, the discharges with added gas puff and lower X-point have larger neutral density in the SOL than the standard case. On the other hand, the discharges with the cryopump on have lower SOL neutral density. The neutral density response inside the separatrix is the opposite to what it is in the SOL. The gas puff and lower X-point discharges have lower neutral density than the standard discharge, while discharges with the cryopump on have higher neutral density. This behavior of the neutrals is caused by the nonlinear character of the fueling dynamics. When gas is puffed, the neutral density in the SOL increases, causing an increase in the particle source. Because of the enhancement in the particle source, the plasma edge density increases. Since the neutral ionization mean free path is inversely proportional to plasma density, the neutral profile inside the separatrix must readjust itself and its decay length becomes shorter. When a steady state is reached, the resulting profiles are such that, in relation to the standard discharge, the neutral density is larger in the SOL and smaller inside the separatrix. In spite of the reduction of neutral density in the edge layer, the particle source remains larger for the gas puff discharges than for the standard discharge. That is, in the edge layer, the increase in plasma density is enough larger than the decrease in the neutral density to increase the core fueling.

For the strong gas puff discharges there is a reduction of neutral density in the region around the X-point, although a secondary peak appears in the poloidal distribution at the gas puff position (top of the chamber). However, the secondary peak is very low (a factor of 10 lower than the peak near the X-point). Because of the change in neutral density, there is a similar change in the charge-exchange damping rate. At the X-point, where we observed the peak of charge-exchange damping rate, its value for the three gas puff discharges is lower by a factor of 5 than the value for the standard discharge.

When the X-point is brought closer to the plate, the neutral density increases close to the X-point, as does the particle source. In this experiment, there is a small increase in the line-averaged density and the edge density when compared with the standard discharge. The edge temperatures are 20% lower. Of course, the conditions for the discharges are not the same, because the power input at the transition is higher in the standard discharge. These discharges with a lower X-point have an enhanced particle source term, with properties similar to a discharge with a very mild gas puff. Therefore, the argument from the case of gas puff discharges carries over to this case.

The argument just presented explains the apparent paradox of increasing the neutral density by gas puff and having a lower power threshold. Furthermore, for these discharges, the charge exchange damping is always lower than the neoclassical damping over the whole poloidal cross section for flux surfaces inside the separatrix. Therefore, we can expect neutrals to play a very small role in the transition, and these discharges should have the lowest power threshold. The discussion of the gas puff discharges can be applied in reverse to the discharges with the cryopump on. For these discharges, the charge exchange damping dominates over the neoclassical damping near the divertor region. Neutrals can play an important role in the cryopump discharges, which have the highest power threshold of all discharges considered.

For the 1994 density scan experiments, the two factors discussed above again play a role in determining the neutral density inside the separatrix: (1) the particle source term which increases as the line-averaged density increases, and (2) the neutral density penetration length, that decreases with increasing line-averaged density. Since the neutral profiles decay toward the inside of the plasma in a quasi-exponential fashion, the reduction in decay length quickly becomes the dominant factor. Therefore, in the inside of the separatrix region, the low line-averaged-density plasma ends up with higher neutral density than the high line-averaged-density plasmas.

3. Discussion and Conclusions

All the experiments analyzed here are at a fixed magnetic field, and the surface area of the separatrix varies very little from one to the other. Therefore, if the increase of power threshold with density is a real plasma physics dependence, $P_{sep}/\overline{n}$ should be essentially a function only of the "hidden" parameters controlling the transition. Hence, we can now look for correlations between $P_{sep}/\overline{n}$ and parameters linked to neutral effects. In the following discussion, we express power in MW, and density in units of 10^{20} m^{-3}. For averaged radius in the region $0.9 > r/r_S > 0.95$, we have found good correlation of $P_{sep}/\overline{n}$ with either the charge-exchange damping rate or the neutral density. It is useful to consider dimensionless parameters representing the effect of neutrals. Since a mechamism possibly responsible for the neutrals' effect on the transition threshold is a change in the damping of the poloidal component of the $E\times B$ shear flow, we consider the parameter $(\nu_{CX})_M/\mu_{neo}$. Here $(\nu_{CX})_M$ is the maximum value of the charge exchange damping rate on a fixed flux surface. In Figure 1, we have plotted $P_{sep}/\overline{n}$ as a function of $(\nu_{CX})_M/\mu_{neo}$ for the $r/r_S = 0.95$ surface. The correlation is very good considering the scattering of the initial data. A fit to the data gives $P_{sep} = \overline{n}\left[0.37 + 0.63(\nu_{CX})_M^2/\mu_{neo}^2\right]$. Since $(\nu_{CX})_M/\mu_{neo}$ increases (decreases) with decreasing (increasing) line-averaged density. The combination of $\overline{n}$ increasing and $(\nu_{CX})_M/\mu_{neo}$ decreasing gives a U-shape dependence for P_{sep} as a function of $\overline{n}$. This dependence is simlar to the one observed in the threshold density scan experiments. The goodness of the fit does not depend strongly on the density scaling assumed for the power threshold, taking $P_{sep} \propto \bar{n}^{\alpha}$ with $1.3 > \alpha > 0.6$ we obtain equally good fits.

A good correlation is also obtained between $P_{sep}/\bar{n}$ and λ_n/r_S, where, λ_n is the poloidally averaged neutral profile radial decay length (from the separatrix inwards). However, such a fit gives a weak U-shape dependence of the power threshold on density. Other parametric dependences are possible. However, having studied experiments from only a single device, it is not possible to discriminate among these possible parameters. Neither is it possible from data correlations to resolve whether the neutrals are the cause or just a reflection of some other mechanism.

We have also tested the correlation of the neutrals with the edge plasma parameters at the transition. For both ion and electron temperature, we have also found good correlation with the normalized charge-exchange damping rate, $(\nu_{CX})_M/\mu_{neo}$, in the same radial region as for $P_{sep}/\bar{n}$. The threshold edge electron density shows an increasing trend with $(\nu_{CX})_M/\mu_{neo}$.

Among other possible correlations between local plasma edge and neutrals parameters, these data also show a correlation between ν_i^* and n_0/n_e at $r/r_S = 0.95$, as also seen in JT-60U [13], [14]. As can be expected, ν_i^* also correlates well with $(\nu_{CX})_M/\mu_{neo}$ (Figure 2). This correlation may be consistent withthe change of the $\nu_i^* =$ constant threshold criterion [25] when modified by the neutral effects [16]. The mechanism assumed to be responsible for this threshold modification [16] is the momentum loss to neutrals by charge exchange, which is consistent with the foregoing discussion. For the L-to-H transition model from Ref. 18, which includes an additional ion loss through collisions with neutrals, the threshold condition at constant pressure gradient can also result in such a correlation.

Acknowledgments

We gratefully acknowledge A. Mahdavi on the experimental planning of the gas puff and pumping experiments, S. H. Hirshman and D. J. Sigmar for useful discussions on the calculation of neoclassical viscous force, M. Rensink and B. Braams for allowing us to use their numerical tools, and K. H. Burrell, P. H. Diamond, and M. Wade for multiple discussions of neutrals effects.

References

[1] Wagner F, Becker G, Behringer K *et al.* 1982 *Phys. Rev. Lett.* **49** 1408
[2] Burrell K H 1994 *Plasma Phys. and Control. Fusion* **36**, A291 (1994)
[3] Burrell K H, Allen S L, Bramson G *et al.* 1988 *Proc. 12th Int.Conf. on Plasma Physics and Controlled Nuclear Fusion Research* vol 1 (Vienna: IAEA) p 193
[4] Tanga A, Bartlett D, Bures M *et al.* 1988 *Proc.15th EPS Conf. on Controlled Fusion and Plasma Heating*, ed EPS, vol. 12B Part 1 (Dubrovnik: EPS) p 235
[5] Ryter F, Stroth U, Wagner F *et al.* 1992 *Proc. 19th EPS Conf. on Controlled Fusion and Plasma Physics* ed K L W Freysinger, R Schrittwieser, W Lindinger, vol 16C, Part I (Innsbruck: EPS), p. 1195
[6] Kardaun O, Ryter F, Stroth U *et al.* 1992 *Proc. 14th Int.Conf. on Plasma Physics and Controlled Nuclear Fusion Research* , vol 3, (Vienna: IAEA) p 251
[7] Ryter F and H mode database working group 1996 *Nucl. Fusion* **36** 1217
[8] Takizuka T, Boucher D, Bracco G *et al.* 1996 *16th IAEA Fusion Energy Conf.* (Vienna: IAEA)
[9] ASDEX Team 1989 *Nucl. Fusion* **29** 1959
[10] Carlstrom T N, Gohil P, Watkins J G *et al.* 1994 *Plasma Phys. Control. Fusion* **36** A147
[11] Mahdavi M A, Brooks N, Buchenauer D *et al.* 1990 *J. Nucl. Materials* **176&177** 32
[12] Shimada M and JT-60 Team, 1992 in *Proc. 14th Int. Conf. on Plasma Physics and Controlled Nuclear Fusion Research* vol. 1 (Vienna: IAEA) p. 57
[13] Tsuchiya K, Takenaga H, Fukuda T *et al.* 1996 *Plasma Phys. Control. Fusion* **38** 1295
[14] Fukuda T, Sato M, Takizuka T *et al.* 1996 *Sixteenth IAEA Fusion Energy Conference* (Vienna: IAEA)

[15] Shaing K C 1993 *Phys. Fluids B* **5** 3841
[16] Shaing K C and Hsu C T 1995 *Phys. Plasmas* **2** 1801
[17] Carreras B A, Diamond P H, and Vetoulis G 1996 *Phys. Plasmas* **3** 4106
[18] Toda S, Itoh S-I, Yagi M *et al.* 1997 *Plasma Phys. Control. Fusion* **39** 301
[19] Leonov V M and Polevoj A R 1994 *Proc. 15th Int. Conf. on Plasma Physics and Controlled Nuclear Fusion Research* vol 3 (Vienna: IAEA) p. 315
[20] Groebner R J, Carlstrom T S, Burrell K H *et al.* 1996 *16th IAEA Fusion Energy Conf.* (Vienna: IAEA).
[21] Carreras B A, Owen L W, Maingi R *et al.* 1997 *Phys. Plasmas*
[22] Carlstrom T N and Groebner R J 1996 *Phys. Plasmas* **3** 1867.
[23] Braams B J 1996 *Contrib. Plasma Phys.* **36** 276
[24] Heifetz D B, Post D, Petravic M *et al.* 1982 *J. Comp. Phys.* **46** 309
[25] Shaing K C, Crume J E C, and Houlberg W A 1988 *Comments Plasma Physics and Controlled Fusion* **12** 69

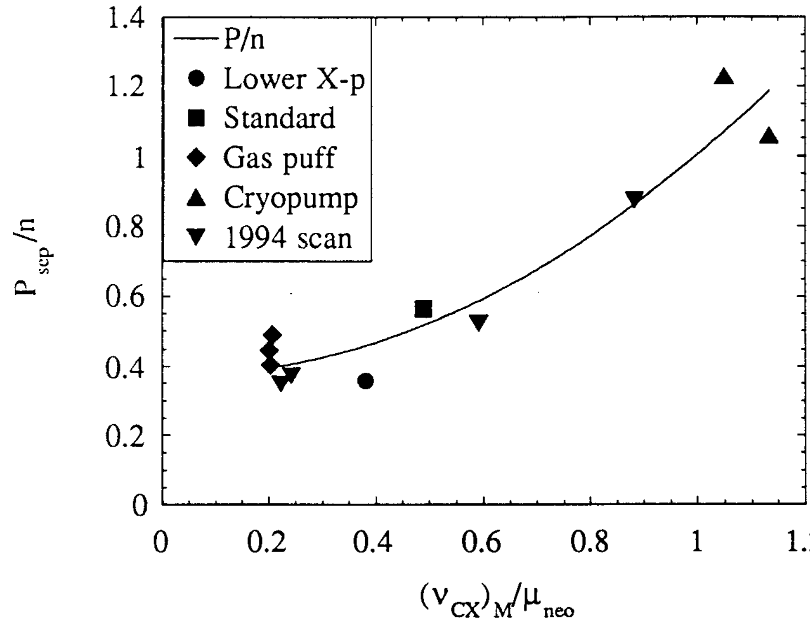

Figure 1. $P_{sep}/\overline{n}$ as a function of $(\nu_{CX})_M/\mu_{neo}$ for the $r/a = 0.95$ surface.

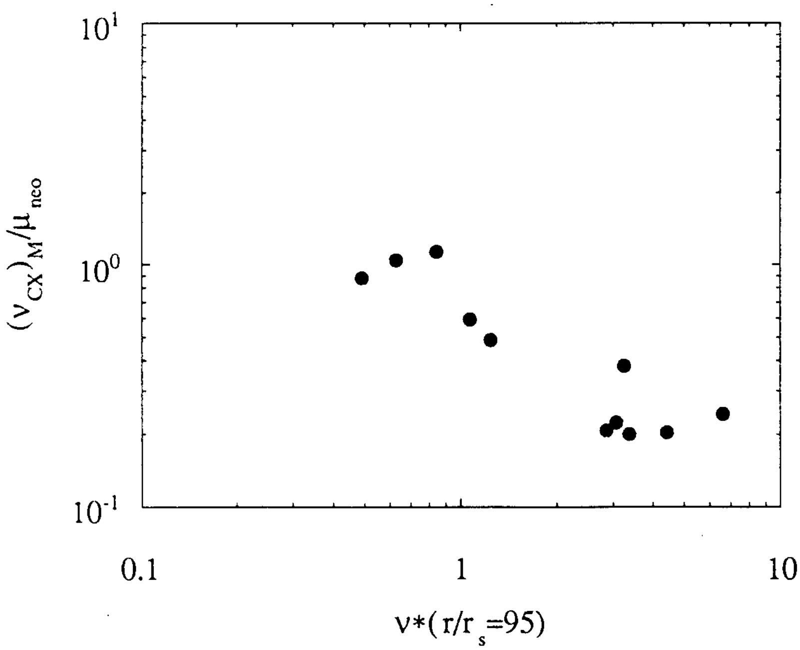

Figure 2. $(\nu_{CX})_M/\mu_{neo}$ as a function of ν^*_i at the $r/a = 0.95$ surface.

M98000334

Report Number (14) ORNL/CP--94439
CONF-9709100--

Publ. Date (11) 199709

Sponsor Code (18) DOE/FE, XF

UC Category (19) UC-101, DOE/ER

DOE